

RESEARCH ARTICLE

Development of Diagnostic Techniques for Early Rheumatoid Arthritis Using Positron Emission Tomography with [^{11}C]PK11195 and [^{11}C]Ketoprofen Tracers

Satoshi Nozaki¹, Naoko Ozaki,² Shinobu Suzuki,² Miki Goto,¹ Aya Mawatari,¹ Yuka Nakatani,¹ Emi Hayashinaka,¹ Yasuhiro Wada,¹ Hisashi Doi,¹ Yasuyoshi Watanabe^{1,3}

¹RIKEN Center for Life Science Technologies, 6-7-3 Minatojima Minamimachi, Chuo-ku, Kobe, Hyogo, 650-0047, Japan

²Department of Molecular and Cellular Biology, Kobe Pharma Research Institute, Nippon Boehringer Ingelheim Co., Ltd, Kobe, Hyogo, Japan

³Department of Physiology, Osaka City University Graduate School of Medicine, Osaka, Japan

Abstract

Purpose: In vivo detection of pathological insults during the early stages of rheumatoid synovitis is essential to allow early anti-inflammatory treatment for prevention of joint destruction. Whether rheumatoid synovitis pathology and the efficacy of therapies can be visualized by positron emission tomography (PET) tracers specific to the inflammatory process was investigated.

Procedures: Using a collagen-induced experimental rat model of rheumatoid arthritis, in vivo imaging using the PET tracers [^{11}C]PK11195, which binds to the translocator protein mainly expressed on myeloid cells, and [^{11}C]ketoprofen, for cyclooxygenase imaging, was performed. To evaluate therapeutic efficacy, model animals were administered the tumour necrosis factor alpha blocker etanercept subcutaneously.

Results: [^{11}C]PK11195 and [^{11}C]ketoprofen uptakes were significantly higher in inflamed paws of collagen-induced arthritis rats than in normal rats. The data showed a correlation between tracer uptake values and paw swelling. After treatment with etanercept, [^{11}C]ketoprofen uptake was significantly lower in treated animals than in untreated ones, whereas [^{11}C]PK11195 uptake in the inflamed regions was comparable to that in the untreated group.

Conclusions: With [^{11}C]PK11195 and [^{11}C]ketoprofen tracers, non-invasive in vivo PET imaging for rheumatoid synovitis can provide diagnostic evidence of early synovitis and allow monitoring inflammatory cell activity during treatment.

Key Words: Rheumatoid arthritis, Early diagnostic techniques, Positron emission tomography, Cyclooxygenase, Translocator protein

Introduction

Rheumatoid arthritis (RA) is an inflammatory disease associated with progressive joint destruction. Currently, the initial phase of RA is known to provide a window of therapeutic opportunity [1] and early diagnosis followed by aggressive treatment of RA might

alter the natural history of RA [2]. Positron emission tomography (PET) is one of the promising imaging techniques for investigation of RA. Previous studies have shown that 2-deoxy-2- ^{18}F fluoro-D-glucose (^{18}F FDG) is useful for visualizing active arthritis [3, 4]. However, ^{18}F FDG-PET detects the cells with specific changes in glucose metabolism and cannot be a specific tracer for the dynamics of inflammation. For example, regenerating damaged tissues, such as myofibroblasts and intestinal stem cells, actively accumulated ^{18}F FDG [5]. Thus, there is a strong demand for tracers that are specific for detecting the pathogenesis of inflammation itself and/or the dynamics of inflammatory cells at disease lesions.

^{11}C PK11195 is a ligand that binds to the 18-kDa translocator protein (TSPO), previously known as peripheral benzodiazepine receptor, mainly expressed on macrophages and monocytes, and TSPO is also known to be up-regulated in activated macrophages [6, 7]. It has been reported that activated macrophages infiltrate into synovial tissues during the early development of RA [8], thus ^{11}C PK11195 may be a promising tracer to follow the dynamics of macrophages in RA joint lesions.

^{11}C ketoprofen is a ligand that binds to cyclooxygenase (COX) 1 and COX2. COXs are enzymes responsible for the formation of prostanoids (i.e., prostaglandins, prostacyclin, thromboxane) that cause the pain and swelling by inflammation [9]. COX1 is constitutively expressed, whereas COX2 is induced by various pro-inflammatory cytokines including tumour necrosis factor alpha (TNF- α). In the early period of osteoarthritis, COX2 is highly expressed in the synovial tissue [10], as in RA [11]. Therefore, ^{11}C ketoprofen can also be a useful tool for monitoring the status of inflammation.

In this study, we evaluated whether the PET imaging technique with ^{11}C PK11195 and ^{11}C ketoprofen can detect the joint destruction in the early phase of RA model rats and furthermore examined whether it assesses monitoring of inflammatory cell activity during treatment.

Materials and Methods

Collagen-Induced Arthritis (CIA) Model

Female Lewis rats were obtained from CLEA Japan, Inc. (Tokyo, Japan). All experimental protocols were approved by the Animal Care and Use Committee of RIKEN Kobe Institute (MAH21-20-1) and were performed in accordance with the National Institutes of Health principles of laboratory animal care [12].

Six-week-old rats were immunized on day 0 with 1 ml of emulsion containing 800 μg of bovine type II collagen (Collagen Gijutsu Kensyukai, Tokyo, Japan) and 200 μg of *N*-acetylmuramyl-L-alanyl-D-isoglutamine hydrate peptide (MDP, Peptide Institute, Inc., Osaka, Japan) by more than ten intradermal injections on the back. A booster injection was given on day 7 with 0.12 ml of the same concentration as on day 0 into the hip region close to the tail. Swelling of the hind

paw was assessed just before PET imaging study by plethysmography (Muromachi Kikai Co., Ltd., Tokyo, Japan).

Treatment with etanercept (Amgen/Pfizer/Takeda) (10 mg/kg, s.c., three times a week) was started on day 14 after the first immunization, and rats were examined by PET on day 28.

CT Scan and Three-Dimensional Analyses

High-resolution in vivo micro-computed tomography (CT) (Inveon, Siemens, Knoxville, TN, U.S.A.) was used to scan the ankle joints of the rat. The animals were placed under anaesthesia with 1.5 % isoflurane. Each joint was scanned at an isotropic resolution of 50 μm at a voltage of 55 kVp and a current of 500 μA , with cone beam mode. For measuring joint destruction, 3D images were constructed using RATOC 3D Medical Image Processing software (RATOC System Engineering Co., Ltd., Tokyo, Japan) into DICOM files. The joint destruction was assessed by visual analysis.

Radiosynthesis

Carbon-11-labelled ketoprofen was synthesized using a rapid carbon-11 methylation method recently developed by our group [13]. The specific radioactivity of ^{11}C ketoprofen was 26.0 ± 5.3 GBq/ μmol at the time of administration. Carbon-11-labelled (*R*)-*N*-methyl-*N*-(1-methylpropyl)-1-(2-chlorophenyl)-isoquinoline-3-carboxamide (^{11}C PK11195) was synthesized according to the method described by Shah et al. [14], with slight modifications. The specific activity was 77.2 ± 34.4 GBq/ μmol at the time of administration. For both tracers, the radiochemical and chemical purities were greater than 99 % as determined by high-performance liquid chromatography.

PET Data Acquisition

The rats were anaesthetised with 1.5 % isoflurane and placed on the bed of the microPET Focus 220 (Siemens, Knoxville, TN, U.S.A.). The absolute sensitivity of the microPET Focus 220 is 2.28 % at the centre of field of view (CFOV) for an energy window of 350–650 keV. The spatial resolution of the system is 1.75 mm at the reconstruction of Fourier rebinning algorithm (FORE) and two-dimensional (2D) filtered back projection (FBP) for an energy window of 250–750 keV [15]. ^{11}C ketoprofen or ^{11}C PK11195 (50 MBq per animal, $N = 4$ each groups) dissolved in 0.5 ml of saline was injected via the cannula inserted into the tail vein, and emission data were then acquired for 90 min using a 3D list-mode method. The data were reconstructed with two-dimensional filtered back projection (ramp filter, cut-off frequency at 0.5 cycles per pixel). For region of interest (ROI) definition and further analysis, summed images (5–90 min post-injection) were reconstructed. ROIs

were drawn on several areas of the synovial tissue in the knee joint of hind paw. Regional uptake of radioactivity in the hind paw was decay-corrected to the injection time and expressed as the standardized uptake value (SUV), where $SUV = \text{tissue radioactivity concentration (MBq/cm}^3\text{)} / \text{injected radioactivity (MBq)} \times \text{body weight (g)}$.

Histological Analysis

The rats were deeply anaesthetised by pentobarbital and perfused transcardially with ice-cold 0.9 % saline followed by 4 % paraformaldehyde solution. Their hind paws were removed and fixed with 4 % paraformaldehyde solution for more than 24 h, decalcified with decalcifying solution B (EDTA method) (Wako Pure Chemical Industries, Ltd., Osaka, Japan) for 10 days and then embedded in optimal-cutting-temperature compound. Serial coronal sections (5 μm) were obtained with a microtome and thaw-mounted on glass slides. For immunostaining, the antibodies used in this study were rabbit IgG (1:200; Cayman Chemical, Ann Arbor, Michigan, USA) for COX-1, rabbit IgG (1:500; Abcam, Cambridge, U.K.) for COX-2 and rabbit IgG (1:1000; developed in our laboratory) for the 18-kDa translocator protein.

Statistical Analysis

Statistical analysis was performed using Student's *t* test. *P* values less than 0.05 were considered significant. Data were shown as mean \pm SD.

Results

Inflammation in the Joints of the RA Model Before Joint Destruction

Whether the animal model of RA can reflect the disease course of RA from the early inflammatory phase, which leads bone destruction, was investigated using in vivo CT analysis on collagen-induced arthritis (CIA) model rats. Figure 1 shows the morphological analysis of the hind paws of the CIA model rats. At 56 days after immunization, the joint destruction had dramatically progressed in immunized rats compared with control. On the other hand, 28 days after immunization, immunized rats showed no notable difference with unimmunized ones. Based on this study, it was confirmed that bone destruction did not occur up to 28 days after disease induction in the rat CIA model. Hence, to clarify the pathogenesis of early inflammatory phase in RA, it is preferable that animal experiment using CIA model rat should be performed up to the first 28 days after immunization.

[¹¹C]PK11195 Accumulation in the CIA Model

To evaluate how [¹¹C]PK11195 PET depicts arthritis during the progress of the disease, PET imaging of CIA rats was performed (Fig. 2a). Rats developed arthritis 14 days after CIA induction, and severe joint swelling occurred by day 21 (volume of paw swelling was $61 \pm 10\%$ compared to control animals; Fig. 2b). The PET image of control rats showed no marked [¹¹C]PK11195 accumulation in the joints (SUV 1.40 ± 0.13 ; Fig. 2c). At day 14, the swollen joints were clearly visualized by PET (SUV 1.47 ± 0.16 ; Fig. 2c) in immunized rats. The accumulation of [¹¹C]PK11195 in the talocalcaneal joints was further increased by day 21 (SUV 1.62 ± 0.07 ; Fig. 2c), and it was slightly decreased at day 28 (SUV 1.51 ± 0.15 ; Fig. 2c). There was a high correlation between tracer uptake (SUV) and the level of paw swelling ($R^2 = 0.93$; Fig. 2d). From these data, the accumulation of [¹¹C]PK11195 was detected in inflamed joints and was associated with the level of paw swelling.

[¹¹C]Ketoprofen Accumulation in the CIA Model

Next, how [¹¹C]ketoprofen PET depicts arthritis during the progress of the disease was evaluated. As shown in Fig. 3a, rats developed arthritis about day 14 after CIA induction and developed severe swelling in the joints by day 21 (the level of paw swelling was 54 ± 9.8 ; Fig. 3b). Then, a tracer uptake study of the joints using [¹¹C]ketoprofen PET was performed, and representative images are shown in Fig. 3a. The PET images of control rats showed no marked [¹¹C]ketoprofen accumulation in their joints (SUV 0.84 ± 0.10 ; Fig. 3c). On day 14, when the disease symptoms were readily recognized, the accumulation of [¹¹C]ketoprofen was clearly visualized by PET (SUV 1.24 ± 0.16 ; Fig. 3c). Its accumulation in the talocalcaneal joints was further increased by day 21 (SUV 1.33 ± 0.46 ; Fig. 3c). On day 28, the accumulation was slightly decreased, and the swelling of joints was also reduced (SUV 1.23 ± 0.26 ; Fig. 3c). There was a moderate correlation between tracer uptake (SUV) and the level of paw swelling ($R^2 = 0.77$; Fig. 3d). From this study, it was shown that [¹¹C]ketoprofen accumulated in inflamed joints along with the development of paw swelling, as seen with [¹¹C]PK11195.

Effect of TNF Inhibitor Treatment on Tracer Accumulation

To evaluate the behaviour of both tracers in the joints after treating the CIA rats with the anti-TNF α blocker etanercept, PET studies with [¹¹C]PK11195 and [¹¹C]ketoprofen were performed before and after treatment. The paw swelling was significantly decreased by anti-TNF α treatment compared with the untreated group (Fig. 5a), and the accumulation of [¹¹C]ketoprofen was also markedly decreased along with paw swelling decrease (Figs. 4b and 5b). In contrast, accumulation

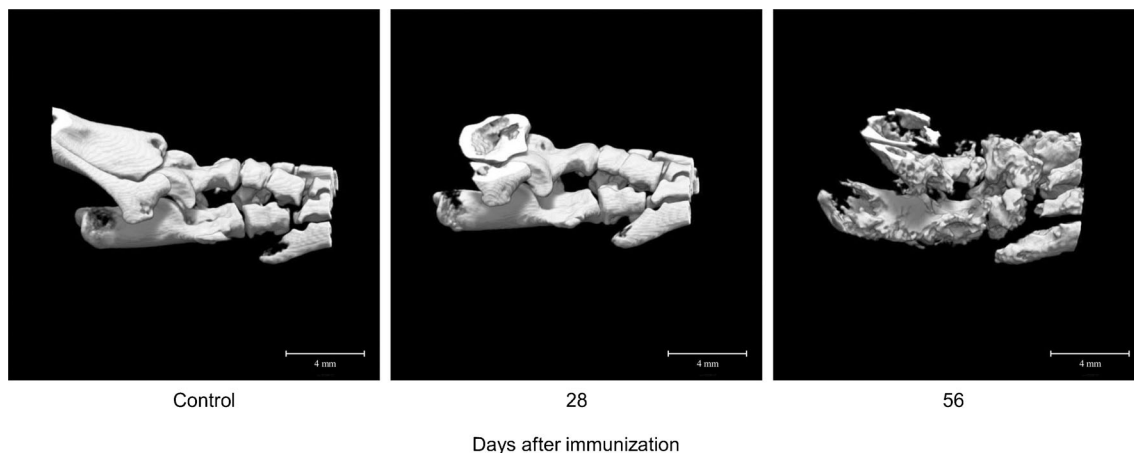


Fig. 1. 3D CT image analysis of the hind paw in CIA model rats. Rats were scanned by high-resolution in vivo micro-computed tomography (Inveon CT) at 0 (control), 28 and 56 days after immunization of bovine type II collagen. Then, two-dimensional images were reconstructed to three-dimensional images. The joint destruction was assessed by visual analysis.

of [¹¹C]PK11195 was still observed even after treatment, and its accumulation level was comparable with that in untreated CIA animals (Figs. 4a and 5a).

Histological Analysis of CIA Model In the rat CIA model, after anti-TNF α treatment, TSPO-immunopositive cells were only slightly decreased, although dramatic reductions in the

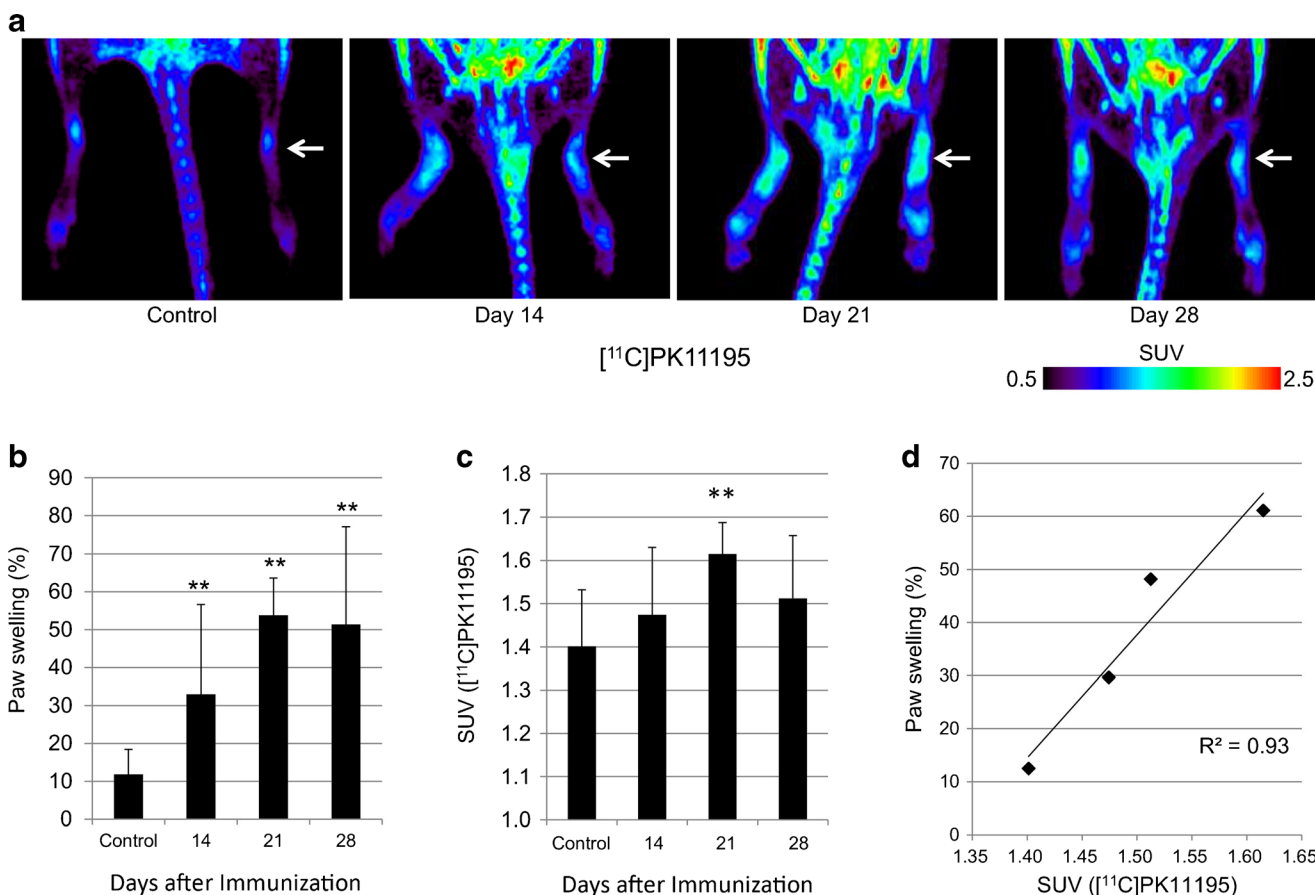


Fig. 2. Increased accumulation of [¹¹C]PK11195 in the hind paw of a CIA rats. **a** [¹¹C]PK11195 PET image shows time-dependent accumulation in the inflamed joint (*white arrow*). **b** Paw swelling and **c** tracer uptake value (SUV) of CIA rats in the hind paw. **d** The correlation analysis of the tracer uptake value (SUV) and paw swelling. Data are shown as mean \pm SD. ** $p < 0.01$, $N = 4$ animals for each groups.

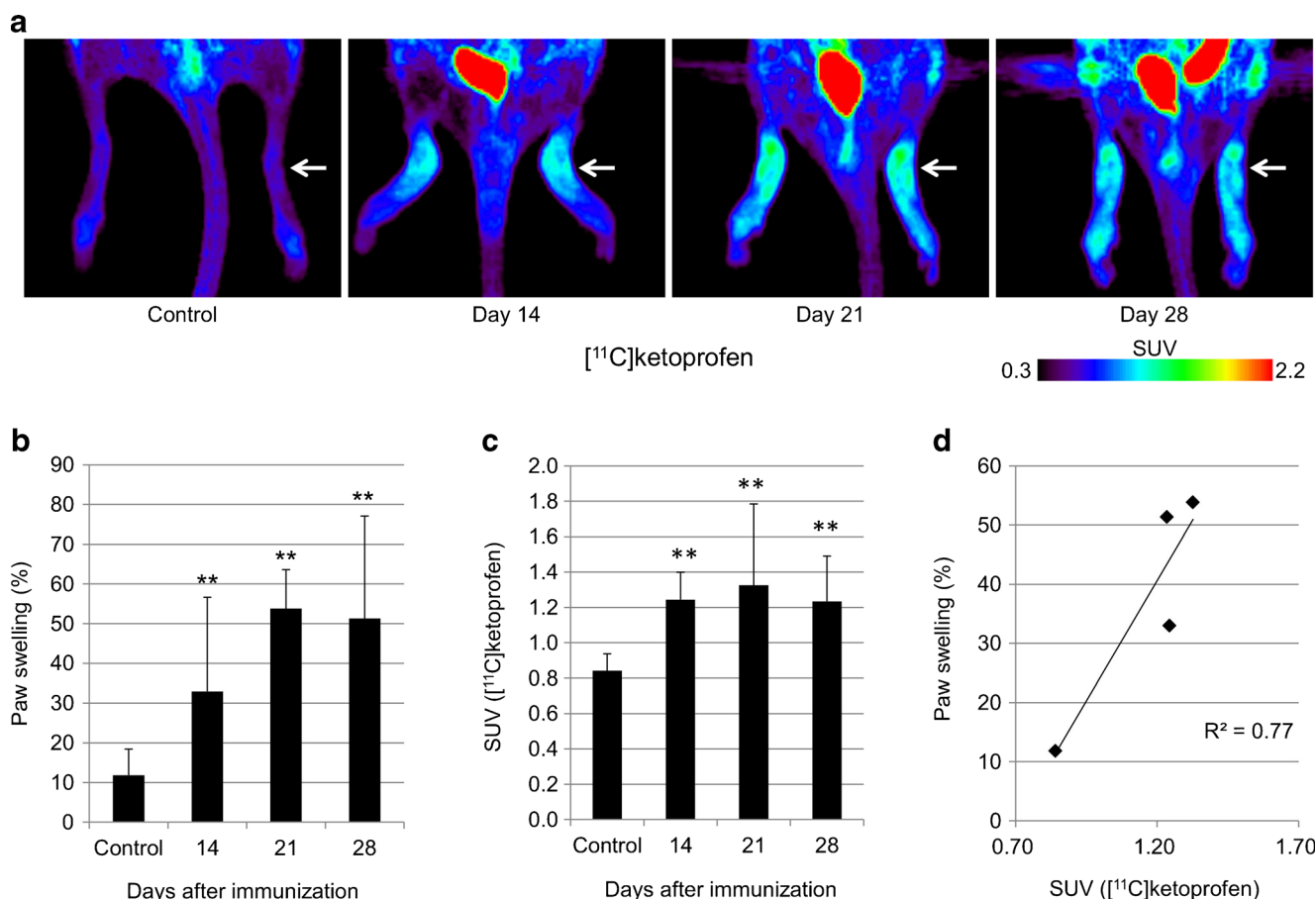


Fig. 3. Increased accumulation of [¹¹C]ketoprofen in the hind paw of CIA rats. **a** [¹¹C]ketoprofen PET image shows time-dependent accumulation in the inflamed joint (*white arrow*). **b** Paw swelling and **c** tracer uptake value (SUV) in the hind paw of a CIA rats. **d** The correlation analysis of the tracer uptake value (SUV) and paw swelling. Data are shown as mean ± SD. ** $p < 0.01$, $N = 4$ animals for each groups.

numbers of COX-2 immunopositive cells were observed. Moreover, on haematoxylin and eosin (HE) staining, massive macrophage infiltration and drastic joint destruction in synovial tissues were observed in the rat CIA model. The joint destruction was not improved by treatment (Fig. 6).

Discussion

This study demonstrated that non-invasive in vivo PET imaging for rheumatoid synovitis using [¹¹C]PK11195 and [¹¹C]ketoprofen can provide diagnostic evidence of early synovitis, allow monitoring of inflammatory cell activity during the progress of the disease and show characteristic changes after treatment.

Inflammation is a major factor driving the progression of structural damage in RA [16], and disease duration has been the most important predictor of response to treatment [17, 18]. Early diagnosis is essential, because initiating aggressive disease-modifying anti-rheumatic drug (DMARD) therapy can improve clinical outcomes in RA patients, including reduction of long-term radiographic progression [19]. In clinical practice, plain radiography is frequently

used to diagnose and monitor RA. However, this method is not sufficient to detect early RA before bone destruction occurs.

PET imaging technique is highly sensitive for detecting the biochemical changes in the joints of RA to capture the disease progression in the early phase of RA. The present study is highly applicable for earlier detection and diagnosis of RA, and this would be a method comparable to biomarker analysis, such as measuring serum amyloid A (SAA), and other imaging technologies, such as ultrasonographic study.

Ketoprofen has a higher affinity to COX1 than to COX2. The 50 % inhibitory concentrations of COX1 and COX2 by ketoprofen in human whole blood cells are 0.047 and 0.24 μ M, respectively [20]. However, the expressions of COX2 are dramatically elevated in synovial blood vessel endothelium, chondrocytes, and subsynovial fibroblast-like cells in RA patients [21]. Immunostaining for COX1 was performed on the synovial tissue of the CIA model rat, but its expression did not change in inflamed joints as compared with the controls (Fig. 6). Therefore, it was assumed that [¹¹C]ketoprofen data mainly reflected a change of COX2 expression. Moreover, the injected mass of [¹¹C]ketoprofen

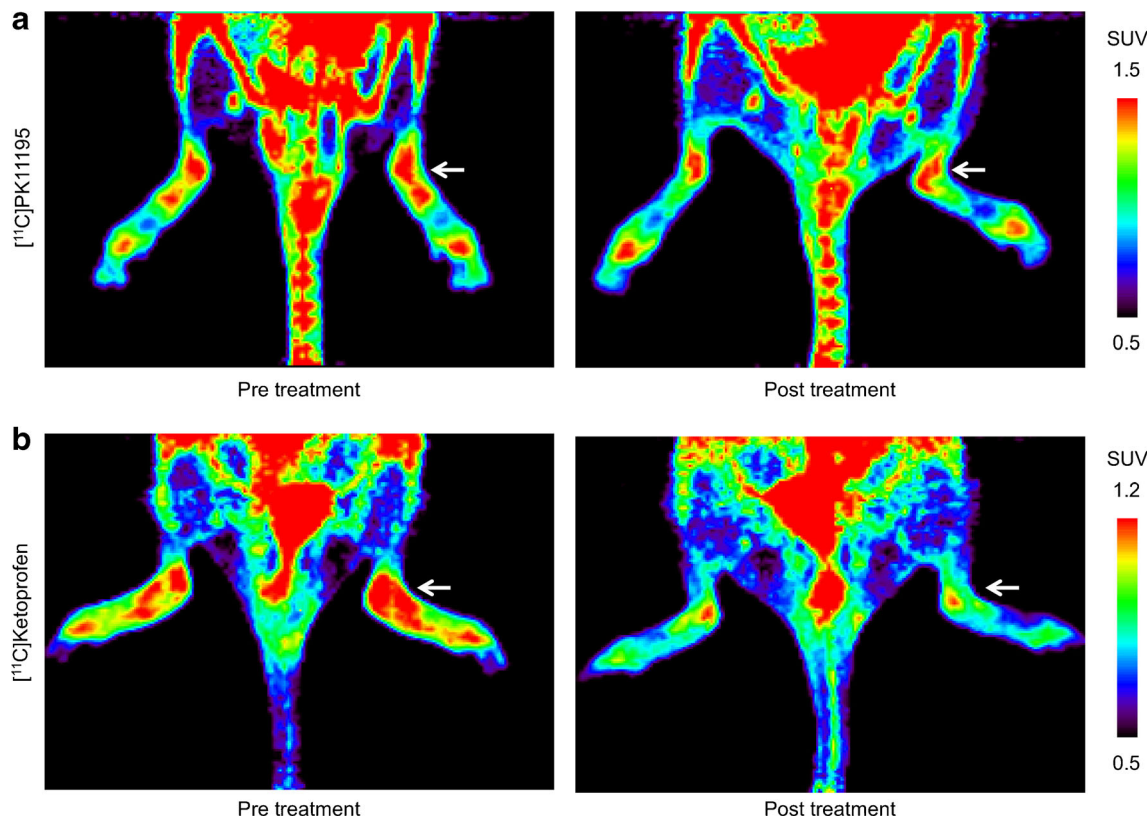


Fig. 4. Effect of TNF α inhibitor treatment on tracer accumulation in the hind paw of CIA rats. **a** [^{11}C]PK11195 and **b** [^{11}C]ketoprofen PET image before and after anti-TNF α inhibitor treatment shows treatment-related change in the inflamed joint (*white arrows*). Tracer uptake value indicated standardized uptake value (SUV).

is ca. 2.0 nmol. So, still, this amount could not reach the problematic concentration of mass effect as compared with the IC₅₀ value of ketoprofen to COX-2 (0.24 μM).

TSPO is up-regulated in activated macrophages [22]. In the present study, [^{11}C]PK11195 was accumulated in the talocalcaneal joints of CIA model rats. In the CIA model, at 21 days after

immunization, many osteoclasts infiltrated the synovial tissue on microscopic observation of HE-stained tissue (Fig. 6). These results indicate that [^{11}C]PK11195 PET depicts inflamed joints. A previous study suggested that PET imaging for TSPO may be useful in the diagnosis of RA patients [23] and subclinical arthritis in anti-citrullinated protein antibody (ACPA)-positive

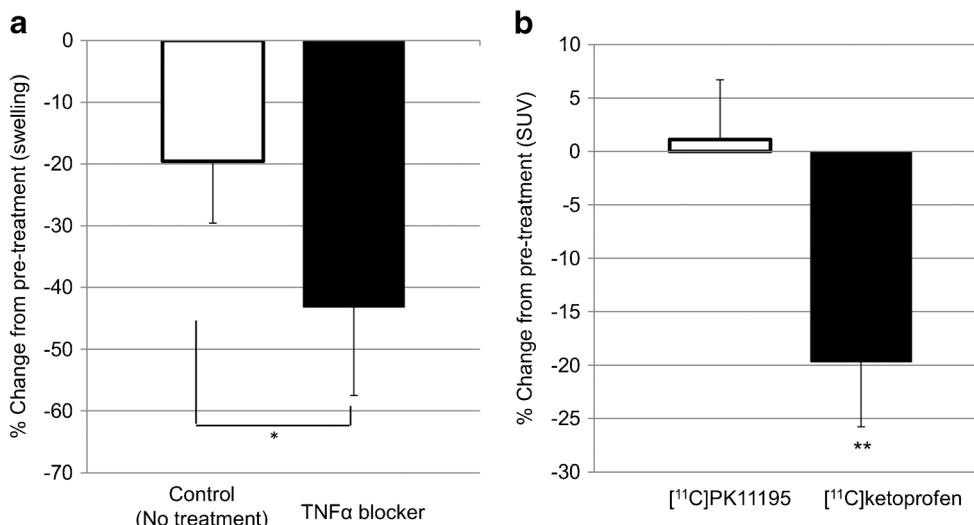


Fig. 5. Effect of anti-TNF α treatment on CIA rats. **a** Percent change from pre-treatment of paw swelling. **b** Percent change from pre-treatment of tracer uptake value (SUV). Data are shown as mean \pm SD. * $p < 0.05$; ** $p < 0.01$, $N = 4$ animals for each groups.

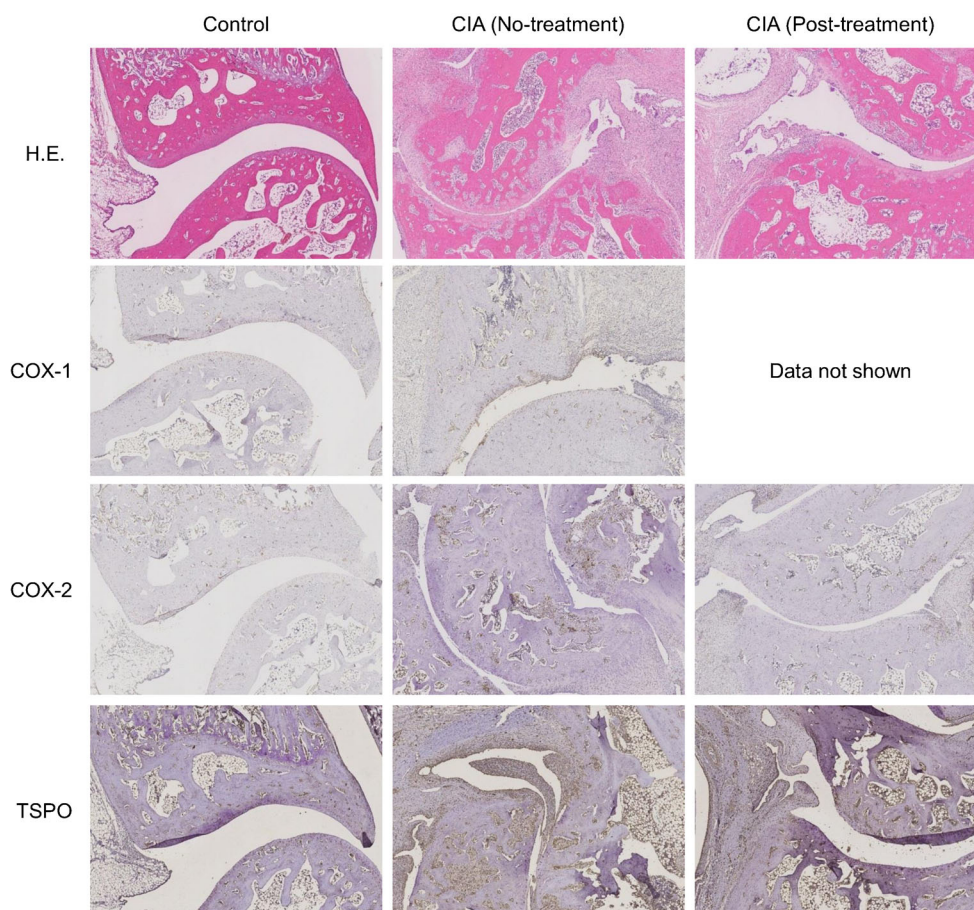


Fig. 6. Histological analysis of joints of CIA rats. Control: CIA control rats; CIA (control [no treatment]): 28 days after CIA induced; CIA (post-treatment): 14 days treatment after 14 days after CIA induced. *HE* haematoxylin and eosin stain, *COX-1* immune-stained with anti-*COX-1* antibody, *COX-2* immune stained with anti-*COX-2* antibody, *TSPO* immune-stained with anti-*TSPO* antibody.

arthralgia patients [24]. Interestingly, in the present study, the accumulation of [^{11}C]PK11195 in the joints of etanercept-treated CIA rats was little changed compared with that in the untreated group. However, paw swelling and the accumulation of [^{11}C]ketoprofen were dramatically reduced in drug-treated rats. This may indicate that macrophages remained in the joints even after the inflammation was diminished after treatment. Etanercept is a human type II $\text{TNF}\alpha$ receptor with Fc protein, but there are several other $\text{TNF}\alpha$ inhibitors, such as infliximab and adalimumab, which are anti- $\text{TNF}\alpha$ antibodies. These antibodies exert complement-dependent cytotoxicity (CDC) activities, which may lead to elimination of activated macrophages, while etanercept showed considerably lower CDC activity [25]. Thus, we speculated that anti- $\text{TNF}\alpha$ antibodies might show different modes of actions compared with etanercept, and [^{11}C]PK11195 would be applicable to understand the variety of clinical effects, not only of these $\text{TNF}\alpha$ inhibitors but of all treatment options.

These tracers would also be very useful to identify local inflammation systematically, enabling us to distinguish synovitis from enthesitis, and they would aid in diagnosing inflammatory diseases other than RA (polyarthritis), such

as oligoarthritis (psoriatic arthritis) and axial arthritis (spondyloarthritis).

Conclusions

PET imaging techniques for diagnosing arthritis using [^{11}C]PK11195 and [^{11}C]ketoprofen were developed. Consequently, non-invasive in vivo PET imaging for rheumatoid synovitis can provide diagnostic evidence of early synovitis and allow monitoring of inflammatory cell activity during treatment.

Acknowledgements. The authors would like to thank Drs. Hitoshi Goto and Kohji Tanaka for their useful advice and comments.

Compliance with Ethical Standards

Conflict of Interest

Naoko Ozaki and Shinobu Suzuki were employees of Nippon Boehringer Ingelheim Co., Ltd. The other authors declare that they have no conflicts of interest. This study was supported in part by a research grant from Nippon Boehringer Ingelheim Co., Ltd., (Tokyo, Japan) to Yasuyoshi Watanabe.

References

1. da Mota LM, Laurindo IM, dos Santos Neto LL et al (2012) Imaging diagnosis of early rheumatoid arthritis. *Rev Bras Reumatol* 52:757–766
2. Cush JJ (2007) Early rheumatoid arthritis—is there a window of opportunity? *J Rheumatol Suppl* 80:1–7
3. Irmiler IM, Opfermann T, Gebhardt P et al (2010) In vivo molecular imaging of experimental joint inflammation by combined ^{18}F -FDG positron emission tomography and computed tomography. *Arthritis Res Ther* 12:R203
4. Kubota K, Ito K, Morooka M et al (2011) FDG PET for rheumatoid arthritis: basic considerations and whole-body PET/CT. *Ann N Y Acad Sci* 1228:29–38
5. Yamato M, Kataoka Y, Mizuma H et al (2009) PET and macro- and microautoradiographic studies combined with immunohistochemistry for monitoring rat intestinal ulceration and healing processes. *J Nucl Med* 50:266–273
6. Canat X, Carayon P, Bouaboula M et al (1993) Distribution profile and properties of peripheral-type benzodiazepine receptors on human hemopoietic cells. *Life Sci* 52:107–118
7. Canat X, Guillaumont A, Bouaboula M et al (1993) Peripheral benzodiazepine receptor modulation with phagocyte differentiation. *Biochem Pharmacol* 46:551–554
8. Kraan MC, Versendaal H, Jonker M et al (1998) Asymptomatic synovitis precedes clinically manifest arthritis. *Arthritis Rheum* 41:1481–1488
9. Vane JR, Bakhle YS, Botting RM (1998) Cyclooxygenases 1 and 2. *Annu Rev Pharmacol Toxicol* 38:97–120
10. Benito MJ, Veale DJ, FitzGerald O et al (2005) Synovial tissue inflammation in early and late osteoarthritis. *Ann Rheum Dis* 64:1263–1267
11. Spangler RS (1996) Cyclooxygenase 1 and 2 in rheumatic disease: implications for nonsteroidal anti-inflammatory drug therapy. *Semin Arthritis Rheum* 26:435–446
12. National Research Council of the National Academies (2011) Guide for the care and use of laboratory animals eighth edition. The National Academies Press, Washington D.C.
13. Takashima-Hirano M, Shukuri M, Takashima T et al (2010) General method for the (11)C-labeling of 2-arylpropionic acids and their esters: construction of a PET tracer library for a study of biological events involved in COXs expression. *Chemistry* 16:4250–4258
14. Shah F, Hume SP, Pike VW et al (1994) Synthesis of the enantiomers of [N-methyl-11C]PK 11195 and comparison of their behaviours as radioligands for PK binding sites in rats. *Nucl Med Biol* 21:573–581
15. Goertzen AL, Bao Q, Bergeron M et al (2012) NEMA NU 4-2008 comparison of preclinical PET imaging systems. *J Nucl Med* 53:1300–1309
16. Emery P, McInnes IB, van Vollenhoven R et al (2008) Clinical identification and treatment of a rapidly progressing disease state in patients with rheumatoid arthritis. *Rheumatology (Oxford)* 47:392–398
17. Möttönen T, Hannonen P, Korpela M et al (2002) Delay to institution of therapy and induction of remission using single-drug or combination-disease-modifying antirheumatic drug therapy in early rheumatoid arthritis. *Arthritis Rheum* 46:894–898
18. Anderson JJ, Wells G, Verhoeven AC et al (2000) Factors predicting response to treatment in rheumatoid arthritis: the importance of disease duration. *Arthritis Rheum* 43:22–29
19. Breedveld F (2011) The value of early intervention in RA—a window of opportunity. *Clin Rheumatol* 30(Suppl 1):S33–S39
20. Warner TD, Giuliano F, Vojnovic I et al (1999) Nonsteroid drug selectivities for cyclo-oxygenase-1 rather than cyclo-oxygenase-2 are associated with human gastrointestinal toxicity: a full in vitro analysis. *Proc Natl Acad Sci U S A* 96:7563–7568
21. Siegle I, Klein T, Backman JT et al (1998) Expression of cyclooxygenase 1 and cyclooxygenase 2 in human synovial tissue: differential elevation of cyclooxygenase 2 in inflammatory joint diseases. *Arthritis Rheum* 41:122–129
22. Folkersma H, Foster Dingley JC et al (2011) Increased cerebral (R)-[(11)C]PK11195 uptake and glutamate release in a rat model of traumatic brain injury: a longitudinal pilot study. *J Neuroinflammation* 8:67
23. van der Laken CJ, Elzinga EH, Kropholler MA et al (2008) Noninvasive imaging of macrophages in rheumatoid synovitis using 11C-(R)-PK11195 and positron emission tomography. *Arthritis Rheum* 58:3350–3355
24. Gent YY, Voskuyl AE, Kloet RW et al (2012) Macrophage positron emission tomography imaging as a biomarker for preclinical rheumatoid arthritis: findings of a prospective pilot study. *Arthritis Rheum* 64:62–66
25. Mitoma H, Horiuchi T, Tsukamoto H et al (2008) Mechanisms for cytotoxic effects of anti-tumour necrosis factor agents on transmembrane tumour necrosis factor alpha-expressing cells: comparison among infliximab, etanercept, and adalimumab. *Arthritis Rheum* 58:1248–1257